


Article

Sluice Gate Design and Calibration: Simplified Models to Distinguish Flow Conditions and Estimate Discharge Coefficient and Flow Rate

Arash Yoosefdoost *  and William David Lubitz

School of Engineering, University of Guelph, Guelph, ON N1G 2W1, Canada; wlubitz@uoguelph.ca

* Correspondence: yoosefdoost@gmail.com

Abstract: Sluice gates are common hydraulic structures for controlling and regulating flow in open channels. This study investigates five models' performance in distinguishing conditions of flow regimes, estimating the discharge coefficient (C_d) and flow rate. Experiments were conducted for different gate openings, flow rates, upstream and downstream conditions. New equation forms and methods are proposed to determine C_d for energy–momentum considering losses (EML) and HEC-RAS models. For distinguishing the flow regimes, results indicated a reasonable performance for energy–momentum (EM), EML, and Swamee's models. For flow rate and discharge coefficient performance of EM, EML, and Henry's models in free flow and for EM and EML in submerged flow were reasonable. The effects of physical scale on models were investigated. There were concerns about the generality and accuracy of Swamee's model. Scaling effects were observed on loss factor k in EML. A new equation and method were proposed to calibrate k that improved the EML model's accuracy. This study facilitates the application and analysis of the studied models for the design or calibration of sluice gates and where the flow in open channels needs to be controlled or measured using sluice gates such as irrigation channels or water delivery channels of small run-of-river hydropower plants.



Citation: Yoosefdoost, A.; Lubitz, W.D. Sluice Gate Design and Calibration: Simplified Models to Distinguish Flow Conditions and Estimate Discharge Coefficient and Flow Rate. *Water* **2022**, *14*, 1215. <https://doi.org/10.3390/w14081215>

Academic Editor: Giuseppe Pezzinga

Received: 1 March 2022

Accepted: 7 April 2022

Published: 10 April 2022

Publisher's Note: MDPI stays neutral with regard to jurisdictional claims in published maps and institutional affiliations.



Copyright: © 2022 by the authors. Licensee MDPI, Basel, Switzerland. This article is an open access article distributed under the terms and conditions of the Creative Commons Attribution (CC BY) license (<https://creativecommons.org/licenses/by/4.0/>).

Keywords: sluice gate; discharge coefficient; flow measurement; hydraulic jump; free hydraulic jump; submerged hydraulic jump; partially submerged hydraulic jump; energy–momentum; design sluice gate

1. Introduction

Sluice is a Dutch word for a channel controlled at its head by a movable gate which is called a sluice gate. A sluice gate can be considered as a bottom opening in a wall [1] or an undershot gate that passes the flow through the bottom, similar to an orifice [2] or a sort of nozzle. The simplicity of sluice gate design, construction, and operation, plus good safety and low maintenance costs [2] result in them being among the most common hydraulic structures to control or measure flow [3].

The volumetric flow rate passing through a sluice gate can be estimated if the opening of the sluice gate (Y_G) and water depths upstream (Y_U) and downstream (Y_D) [2,3] are known. Low head loss and no need for new equipment make sluice gates preferable for measuring the flow rate where a device is installed [3]. However, the accuracy of flow rates calculated based on sluice gate flows is typically less than weirs, and a complex calibration is needed to account for cases of free or submerged hydraulic jumps downstream of the gate [2–5]. The flow under sluice gates can be categorized as a free hydraulic jump (F), partially submerged hydraulic jump (PS), or submerged hydraulic jump (S) [6,7].

Figure 1 shows a sluice gate when a free hydraulic jump occurs. Here, Y_U is the upstream depth, Y_G is the opening of the gate, Y_m is the minimum depth of flow after the sluice gate, Y_{J1} and Y_{J2} are the initial and secondary depths of the hydraulic jump, respectively, and Y_D is the downstream depth.

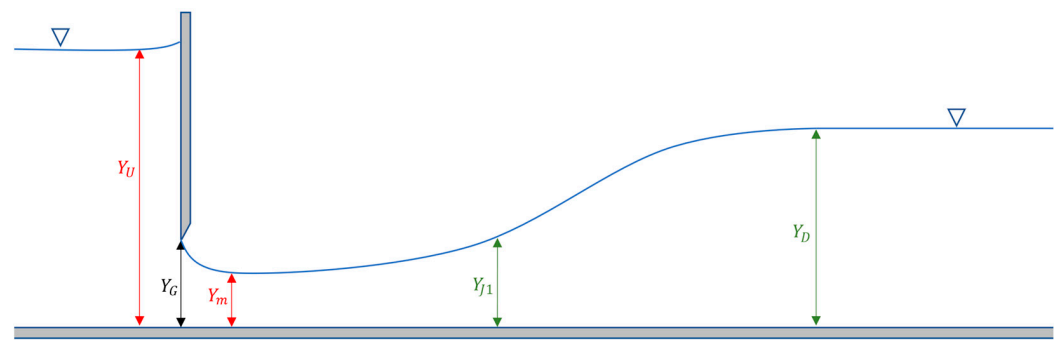


Figure 1. Free hydraulic jump.

Many studies focused on characterizing the free (classic) hydraulic jump [8–12]. The flow after the sluice gate behaves like a stream coming out of an orifice (nozzle) [1]. White (2011) proposed that a free discharge is expected for $Y_U/Y_G > 2$ (or $Y_U > 2 Y_G$) [1]. However, the literature indicates studies that relate the upstream flow depth to the maximum tailwater (downstream) depth to define flow regime distinguishing condition curves [13]. To estimate the volume of flow, many studies focused on determining the coefficient of discharge (C_d). An early, significant study is Henry’s 1950 experiment to estimate the C_d for free and submerged flows [14]. Henry developed a relationship between the C_d and Y_U/Y_G by neglecting energy losses and assuming a uniform velocity and a hydrostatic pressure distribution both upstream and at the vena contracta, providing a practical, widely used graph of this relationship represented in Figure 2 [14]. The highest value of C_d (0.611) occurs in the free flow regime [15].

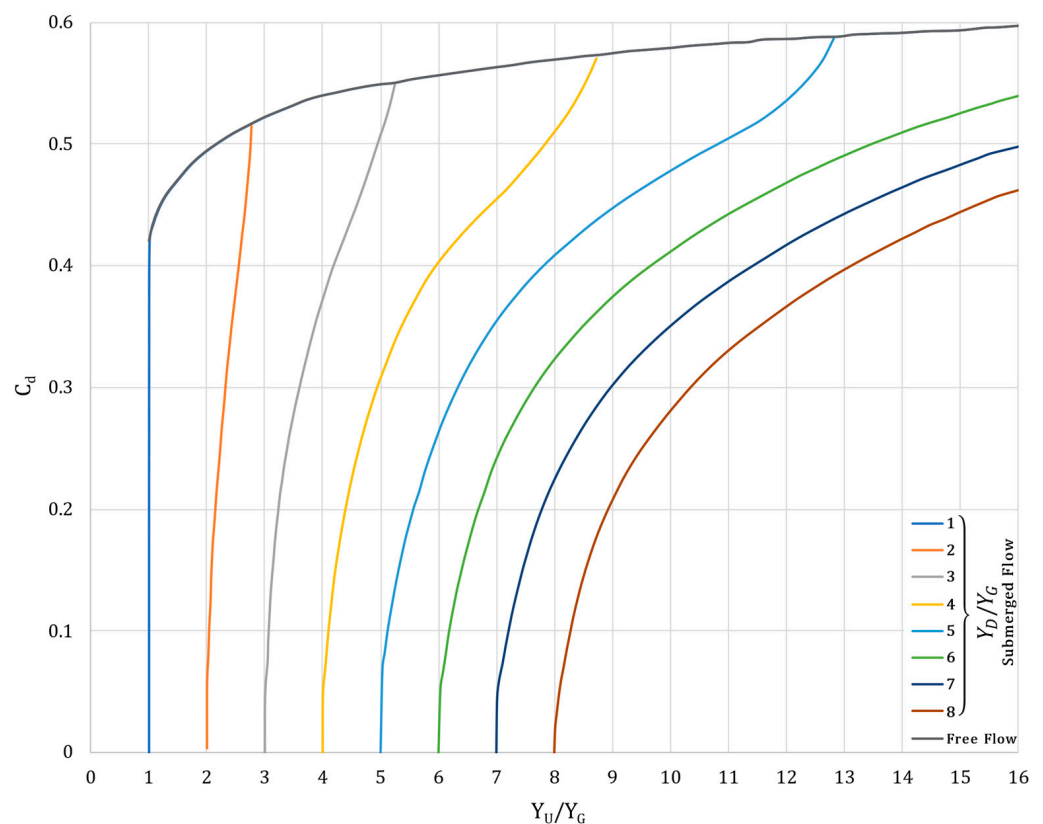


Figure 2. Henry’s 1950 nomograph for the range of C_d for free and submerged flow regimes in sluice gates [15].

In 1967, Rajaratnam and Subramanya used the energy–momentum (EM) method to prove Henry’s (1950) results [10]. In 1992, Swamee developed several relationships for free and submerged flows based on Henry’s (1950) graph [15] to help prevent interpretation errors when interpolating discharge coefficient curves and provide an analytical and/or numerical method for determining the discharge coefficient for sluice gates. Lozano et al. Roth and Hager (in 1999) experimentally studied the effects of viscosity and surface tension on scaling sluice gate operations in free-flow conditions. Their research included studies on the contraction coefficient as well as other parameters such as the distribution of velocity and pressure on the gate and the channel bottom [16].

Lozano et al., in 2009, performed field studies on four rectangular sluice gates by measuring the water depth and gate opening values [12]. They reported that the EM model resulted in reasonable discharge estimations for three of the studied gates by calibrating the contraction coefficient. For the case where the EM method estimations were not accurate, the sluice gate had a unique nonsymmetric flow condition and was located at the channel’s head [17].

Habibzadeh et al., in 2011, applied a theoretical method based on EM equations to find an equation for the discharge coefficient of sluice gates in rectangular channels based on orifice-flow conditions, applicable in both free and submerged flow conditions [18]. In most sluice gate models, the energy losses are assumed negligible; however, Habibzadeh et al. reported that turbulence-related phenomena cause significant energy losses in the submerged-flow condition. Additionally, the recirculating region below the gate induces turbulence that results in energy loss in the upstream pool. They considered the magnitude of an additional energy-loss factor as a function of the sluice gate geometry and proposed that it could affect the discharge coefficient [18].

Some studies divided submerged flow regime into two subcategories: 1. low and 2. high submerged regimes [13]. In 2011, Habibzadeh et al. proposed an equation to calculate a parameter called “transitional value of tailwater depth”, based on several factors, including the contraction coefficient, upstream flow depth, gate’s opening, and an energy loss factor which was considered to be 0.062 [18]. The free-flow regime is expected for downstream water depths less than this value, while a submerged flow regime is expected for higher downstream depths. They also proposed a measure to distinguish the submergence ratio of the flow as a function of the maximum tailwater depth for free flow and the downstream depth. According to this measure, the flow is considered low submerged for submergence ratios between 0 and 20 and considered high submerged for values higher than this range [13,18]. Castro-Orgaz et al., in 2010, proposed that for high submergence situations, the common EM method is not accurate. They proposed a new equation for submerged flow based on the energy–momentum method principles by applying correction factors on velocity and momentum [19]. However, in 2012, Bijankhan et al. showed that this method has significant errors when the submergence is not significant [13]. The analysis of the EM method indicates that the roller momentum flux and the energy loss could be significant. Therefore, in 2013, Castro-Orgaz et al. published a revised version of their 2010 research for estimating sluice gate discharge in submerged conditions. The new method introduces rationality in the EM equations for submerged gate flow. However, the results of this method were similar to the former one [20].

Gumus et al. (2016) studied the velocity field and surface profile of the submerged hydraulic jump of a vertical sluice gate using 2D CFD modeling. The results of this numerical study were compared with experimental data, and they concluded that the accuracy of the Reynolds Stress Model (RSM) is more than other studied turbulence models in predicting horizontal velocities and computing the free-surface profile of the hydraulic jump characteristics [21].

Rady (2016) applied developed multilayer perceptron (MLP) artificial neural networks (ANNs) to predict C_d of vertical and inclined sluice gates. This study applies the MLP using the steepest descent back-propagation training algorithm and one hidden layer. For free flow, ANNs used Y_U/G , the sluice gate’s inclination angle, Froude number and Reynolds

number. For submerged flow, Y_D/G was used in addition to the former inputs. Rady reported that using this method led to reasonable accuracy [22].

Silva and Rijo (2017) studied several methods to determine C_d including EM-bases models, orifice flow rate relationships, and dimensional analysis using Buckingham's Π -theorem. They concluded that the EM-based method led to better results for all free, submerged, and partially submerged flows. Additionally, they reported that there were no improvements in discharge estimation results of the methods that divide the partially and fully submerged flows for the studied sluice gate openings [3].

Kubrak et al. (2020) investigated measuring the volumetric flow rate using sluice gates under submerged flow conditions. A laboratory experiment on a model made on a 1:2 scale of an irrigation sluice gate was conducted to collect the experimental data. This study utilized Swamee's (1992) model as a basis for the determination of C_d . Using this experimental data and empirical methods to adopt corrections, they achieved a reasonable accuracy for estimated discharge coefficients of Swamee's (1992) model for this case study. Based on this and as stated by Boiten (1992) [23], they concluded that this method is useful in estimating flow through the sluice gate [24].

Nasrabadi et al. (2021) compared the Group Method Data Handling (GMDH) and Developed Group Method of Data Handling (DGMDH) machine learning methods to predict the characteristics of a submerged hydraulic jump of a sluice gate. Their study indicated a reasonable accuracy for both models in estimating relative submergence depth, jump length, and relative energy loss [25].

Based on the literature, the flow under the sluice gate is a classic problem that has been extensively studied experimentally and numerically. Hence, the literature indicates that in recent years the advancements in new measurement methods, such as using a laser Doppler anemometer to measure velocity fields [21], etc., improved the accuracy and domain of experimental measurements on this topic. Moreover, beside the classic studies, modern methods such as machine learning techniques, AI, and CFD opened new avenues for investigations on this topic. However, in practice, modern methods are not easy to implement or cost-effective: the new measurement methods are technology-based and require new instruments to be installed, and the application of modern techniques is still highly dependent on the operator's skills and experience.

It is worth mentioning that in practice, some sluice gate models are available in software packages such as SIC and HEC-RAS. The Simulation of Irrigation Canals (SIC) is a one-dimensional hydrodynamic model for river and irrigation canal modeling and regulation [6]. This commercial software has been released by Cemagref since 1989. SIC utilizes empirical relationships [6] based on orifice flow equations [3] to estimate the flow rate under sluice gates. The Hydrologic Engineering Center's River Analysis System (HEC-RAS) has been released since 1995 and supports 1-D steady flow, 1-D and 2-D unsteady flow calculations [7]. However, these software packages cannot estimate C_d . For SIC, some literature suggests considering C_d as 0.6 [26], and the HEC-RAS manual suggests that typically $0.5 \leq C_d \leq 0.7$ [7]. Such a drawback makes the accuracy of results depend on choosing an appropriate value for C_d and the experience of the operators and makes this software not desirable for the design of sluice gates.

In practice, for existing sluice gates, calibration and determination of the optimum C_d is performed using field or experimental measurements. However, models and tools used to characterize flow under sluice gates are essential, especially where the experimental data is not available for calibration, such as for design purposes. On top of that, in system optimization, non-iterative and fast analytical calculations for a component are important for maintaining the overall efficiency of optimizing the whole system of many components. Hence, many available models in the literature still require further investigations, require adequate knowledge to apply, and are not simplified enough or represented in a standard method for such purposes. The essence of developing standard and simple analytical methods is even more significant when sluice gates need to be modeled as a component

in a complex hydraulic system, especially when there are many scenarios to be studied, managed, or optimized.

As a result, this study focused on analyzing, evaluating, and simplifying models to improve the application of the models with higher accuracy in the design of sluice gates. Five models were reviewed, analyzed, represented in a standard and easy to use form, and their performance was evaluated in distinguishing conditions of flow regimes, estimating the C_d and flow rate. For this purpose, a series of lab experiments were conducted at the University of Guelph to study the flow on different sluice gate openings, flow rates, upstream and downstream conditions. The effects of physical scale on models were investigated, and recommendations were provided. Moreover, new analytical equations are proposed to improve the accuracy or applicability of some models. The unscalable initial studies costs are a large burden on small projects [27,28]. The presented new equations and simplified models could facilitate their applicability in the design of sluice gates and initial studies of small projects such as the irrigation channels or pico- and micro-hydropower plants. In addition, this study contributes to simplifying these models in a standard form to facilitate the application of models, particularly for modeling sluice gates as a component in complex hydraulic systems such as hydropower plants. The contributions of the analytical equations and models proposed in this study facilitate the development of models for such complex hydraulic systems for optimization purposes, development of management or operation plans, etc.

2. Methods and Materials

2.1. Models

In order to meet the research goals and to facilitate the application of models for the purposes mentioned above, they were modified and represented in a simplified and standard form. To keep everything concise and to the point, the necessary hydraulic background and fundamental equations used in this research are provided in Appendix A.

2.1.1. Energy–Momentum Model

According to Appendix A, Equation (A3) enables calculating the volumetric flow rate Q using Y_U and Y_m . This equation can be written as:

$$Q = C_d b Y_G \sqrt{2gY_U} \quad (1)$$

where b is the channel width, g is the gravitational acceleration (9.807 m/s^2), C_d is the sluice gate's coefficient of discharge, and for free flow:

$$C_d = \frac{C_c}{\sqrt{1 + \Delta}} \quad (2)$$

where C_c is the contraction coefficient, which is the ratio of the jet width to the orifice opening width [29] or the ratio of the cross-sectional area of the jet vena contracta to its opening area [30]. Therefore, in rectangular channels:

$$C_c = Y_m / Y_G \quad (3)$$

In this study, Δ is defined as the ratio of the alternative depths ($\Delta = Y_m / Y_U$) and using Equation (3), it could be represented as follows:

$$\Delta = C_c Y_G / Y_U \quad (4)$$

A free hydraulic jump (Figure 1) could be expected after the sluice gate if the downstream's conjugate depth is equal to or more than the sluice gate's upstream supercritical alternate depth (i.e., $Y_m \leq Y_{J1}$). In a free hydraulic jump, the jet after the sluice gate rapidly converges to Y_m at the contraction point (the vena contracta), which is the minimum possible flow depth. For $Y_m < Y_{J1}$, the flow velocity decreases due to frictional resistance

in a Gradually Varied Flow (GVF) regime, leading to a gradual increase in flow depth until it reaches the depth, where the hydraulic jump initiates, which is the conjugated depth of downstream depth [31]. For the case where $Y_m = Y_{J1}$ the hydraulic jump forms at cross-section m . Considering the fact that the vena contracta is the minimum possible flow depth, applying Equation (A6) to calculate the conjugate depth of $Y_m = Y_{J1}$, and by substituting Y_m from Equation (3) and q from Equation (A3), the maximum downstream depth for which free flow could be expected (Y_{DMF}) can be calculated as follows:

$$Y_{DMF} = 0.5Y_U\Delta \left(\sqrt{1 + \frac{16}{\Delta(1+\Delta)}} - 1 \right) \tag{5}$$

Equation (5) could be considered as the distinguishing condition for free and submerged flows [32].

Physically, $Y_m > Y_{J1}$ is not possible, and in practice, a submerged hydraulic jump (SHJ) occurs in such a situation. In such a situation, the jump would ordinarily be pushed further upstream, but the sluice gate prevents this, so the upstream conjugate depth cannot be reached, and a submerged (drowned) hydraulic jump forms [31] (Figure 3). For submerged flow, the energy and momentum equations can be re-written by defining the piezometric head Y_P as [3,18]:

$$Y_U + \frac{q^2}{2gY_U^2} = Y_P + \frac{q^2}{2gY_m^2} \tag{6}$$

$$\frac{Y_P^2}{2} + \frac{q^2}{Y_{J1}g} = \frac{Y_{J2}^2}{2} + \frac{q^2}{Y_{J2}g} \tag{7}$$

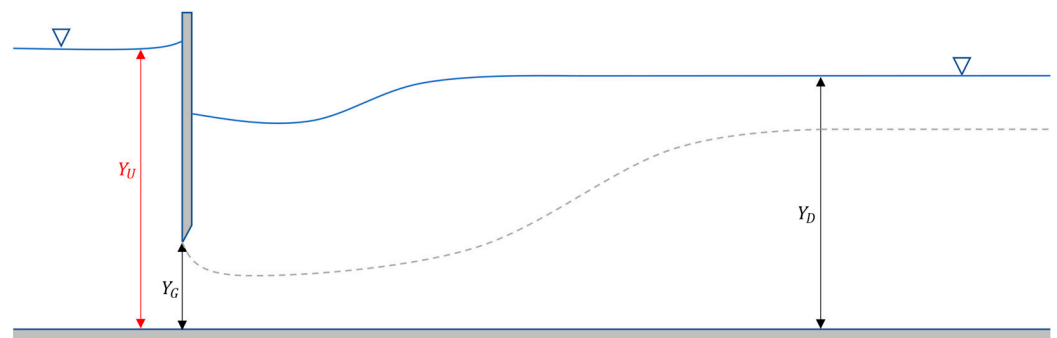


Figure 3. Submerged (drowned) hydraulic jump.

Then, C_d can be found by solving Equations (6) and (7) interactively [33] and eliminating Y_P [32]. Therefore, it can be shown that for submerged flow [32]:

$$C_d = C_c \frac{\Delta}{1-\Delta^2} \sqrt{\sigma - \sqrt{\sigma^2 - \left(\frac{1}{\Delta^2} - 1\right)^2 \left(1 - \frac{1}{\delta^2}\right)}} \tag{8}$$

where

$$\delta = Y_U/Y_D \tag{9}$$

$$\sigma = \left(\frac{1}{\Delta} - 1\right)^2 + 2(\delta - 1) \tag{10}$$

2.1.2. Energy–Momentum Model with Loss

The classic Energy–Momentum (EM) method considers the losses between the upstream and vena contracta negligible. Habibzadeh et al. (2011) proposed that the energy

losses between these sections should be considered by adding the loss term $kV_m^2/2g$ to Equation (A2) [18]:

$$Y_U + \frac{q^2}{2gY_U^2} = Y + K \frac{q^2}{2gY_m^2} \quad (11)$$

where k is the energy loss factor, V_m is the average velocity in the vena contracta, and:

$$K = k + 1 \quad (12)$$

Based on the experimental data of Rajaratnam and Subramanya (1967) [34], Habibzadeh et al. (2011) determined the value of k as:

$$k = \begin{cases} 0.062, & \text{Free flow} \\ 0.088, & \text{Submerged flow} \end{cases} \quad (13)$$

For free flow $Y = Y_m$. Therefore, C_d could be calculated by substituting Equation (1) in Equation (11) to get:

$$C_d = C_c \sqrt{\frac{1 - \Delta}{K - \Delta^2}} \quad (14)$$

For submerged flow $Y = Y_p$ and C_d could be obtained by simultaneously solving Equations (15) and (19). Habibzadeh et al. (2011) reported the physically possible root of the resulting equation [18]. In the current study, we offer a simpler equation with an emphasis on its considerable similarity to Equation (8), which is the result of the EM-based analytical nature of this method:

$$C_d = C_c \frac{\Delta}{K - \Delta^2} \sqrt{\lambda - \sqrt{\lambda^2 - \left(\frac{K}{\Delta^2} - 1\right)^2 \left(1 - \frac{1}{\delta^2}\right)}} \quad (15)$$

where

$$\lambda = \sigma + k/\Delta^2 \quad (16)$$

Similar to the EM method, substituting Equation (12) in Equation (1), then in Equation (A6), leads to finding the maximum tailwater depth for which a free flow could be expected after the sluice gate (Y_{DMF}) that could be used to distinguish free and submerged flow:

$$Y_{DMF} = \frac{\Delta}{2Y_U} \left(\sqrt{1 + \frac{16(1 - \Delta)}{\Delta(K - \Delta^2)}} - 1 \right) \quad (17)$$

Finally, Equation (1) is applied to calculate the volumetric flow rate predicted by the EM with the loss model.

In this study, this model, which is proposed by Habibzadeh et al. (2011), is referred to as EML.

2.1.3. Henry's Model

Henry (1950) proposed the well-known nomograph based on experimental data to estimate C_d for different flow regimes. Additionally, based on the EM model, Henry proposed that for free flow:

$$C_d = \alpha C_c \sqrt{1 - \beta} \quad (18)$$

where Henry assumed $C_c = 0.6$ and [3,14]:

$$\alpha = \frac{1}{\sqrt{1 - \Delta^2}} \quad (19)$$

$$\beta = \begin{cases} \Delta, & \text{Free flow} \\ Y_P/Y_U, & \text{Submerged flow} \end{cases} \tag{20}$$

$$Y_P = C_c Y_G \frac{\alpha^2 + \sqrt{\alpha^4 + 4\eta(\eta(Y_D/Y_G)^2 - \alpha^2(Y_U/Y_G))}}{2\eta} \tag{21}$$

$$\eta = (4C_c(1 - C_c Y_G/Y_D))^{-1} \tag{22}$$

Henry’s (1950) model applies Equation (1) to calculate the volumetric flow rate.

2.1.4. Swamee’s Model

Swamee (1992) applied a nonlinear regression to Henry’s (1950) nomograph and proposed the following range for free flow [15]:

$$Y_U \geq 0.81 Y_D \left(\frac{Y_D}{Y_G}\right)^{0.72} \tag{23}$$

Therefore, the following equation was proposed as the distinguishing condition for free and submerged flows in Swamee’s model based on the maximum downstream depth at which free flow could be expected ($Y_{D_{MF}}$):

$$Y_{D_{MF}} \leq \sqrt[1.72]{\frac{Y_U Y_G^{0.72}}{0.81}} \tag{24}$$

Swamee (1992) considered $C_c = 0.611$ and defined C_d as [15]:

$$C_d = \theta C_c \left(\frac{Y_U - Y_G}{Y_U + 15Y_G}\right)^{0.072} \tag{25}$$

where $\theta = 1$ for free flow, and for submerged flow:

$$\theta = \frac{(Y_U - Y_D)^{0.7}}{0.32 \left(0.81 Y_D (Y_D/Y_G)^{0.72} - Y_U\right)^{0.7} + (Y_U - Y_G)^{0.7}} \tag{26}$$

To calculate the volumetric flow rate, the Swamee (1992) model applies Equation (1).

2.1.5. HEC-RAS Model

The U.S. Army Corps of Engineers’ River Analysis System (HEC-RAS) software is developed for open channel flow computation under steady and unsteady conditions [7]. HEC-RAS does not provide a method to calculate C_d for sluice gates and this coefficient needs to be supplied by the user. The HEC-RAS manual suggests that typically $0.5 \leq C_d \leq 0.7$ [7]. In HEC-RAS, the flow regimes of the sluice gates are categorized based on the ratio of Y_D/Y_U . These ranges are represented in Table 1.

Table 1. HEC-RAS distinguishing range for sluice gate flow regimes [7].

Flow Regime	Free Flow	Partially Submerged Flow	Submerged Flow
Condition	$Y_D/Y_U \leq 0.67$	$0.67 < Y_D/Y_U < 0.80$	$Y_D/Y_U \geq 0.80$

Therefore, the following equation could be proposed as the distinguishing condition based on the maximum downstream depth at which free flow could be expected ($Y_{D_{MF}}$) based on the HEC-RAS model’s definition:

$$Y_{D_{MF}} \leq 0.67 Y_U \tag{27}$$

Similarly, the following equation could be proposed as the distinguishing condition based on the minimum downstream depth at which a submerged flow could be expected ($Y_{D_{ms}}$) based on the HEC-RAS model's definition:

$$Y_{D_{ms}} \geq 0.8 Y_U \quad (28)$$

For other situations ($0.67 Y_U < Y_D < 0.8 Y_U$) partially submerged flow would be expected based on the HEC-RAS model definition.

To calculate the flow rate, HEC-RAS utilizes Equation (1) for free flow, Equation (29) for partially submerged flow, and Equation (30) for submerged flow [3,7]:

$$Q = C_d b Y_G \sqrt{2g 3(Y_U - Y_D)} \quad (29)$$

$$Q = C_d b Y_G \sqrt{2g (Y_U - Y_D)} \quad (30)$$

2.2. Laboratory Flume and Experiment

Experiments were conducted in the Water Resources (Flume) lab of the University of Guelph. The steady-state flow through a sluice gate in a laboratory flume was characterized as a function of various upstream and downstream water depths. Figure 4 shows a schematic view of this laboratory experiment setup. Water is pumped from the main reservoir to a header tank connected to a sluice gate that controls the flow that enters the flume. This laboratory flume is a rectangular channel 0.15 m wide and 0.3 m deep, with a length of 6.12 m. It is made of plexiglass to enable flow visualization. The flume was carefully leveled to produce a channel with zero slope, and an adjustable sharp-edged sluice gate was installed near a point 1/3 of flume length downstream of the flume inlet. The downstream flow depth was controlled by an adjustable weir installed at the outlet of the flume. Water passing over the end weir returns to the main reservoir by gravity through a vertical pipe. A valve is installed in this return pipe to allow diversion of the return flow to a gauged tank calibrated volumetrically to measure the volumetric flow rate.

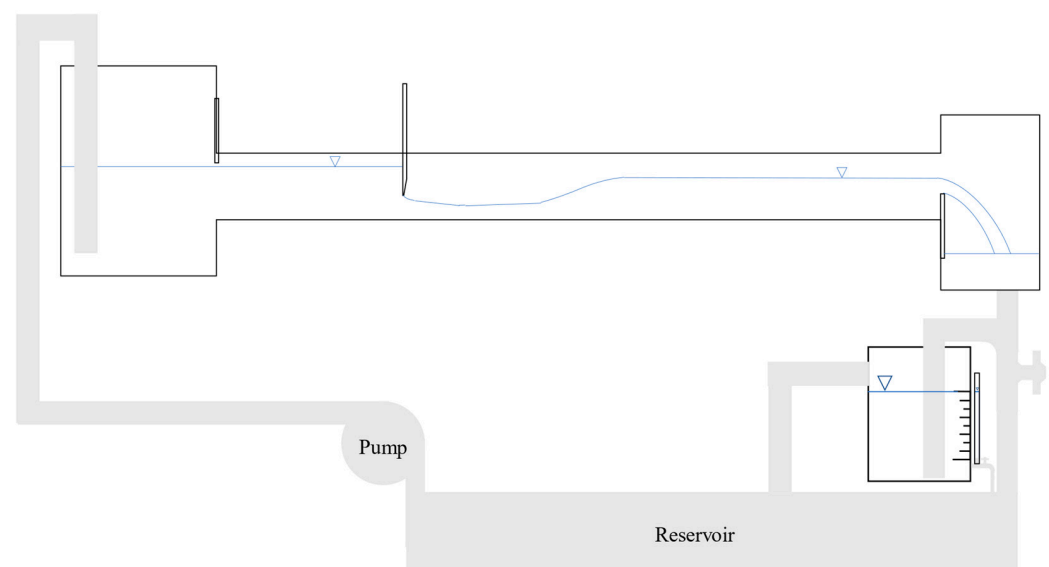


Figure 4. Schematic of the lab experiment configuration (not to scale).

The experiments were performed for target flow rates from 0.5×10^{-3} to $3.0 \times 10^{-3} \text{ m}^3/\text{s}$. For each flow rate, experiments were performed for a set of sluice gate openings from 5 to 100 mm. For each flow rate and sluice gate opening, tests were conducted for the weir

elevations from 0 up to 150 mm. Table 2 summarizes the ranges of flow rates, sluice gate openings, and weir heights tested.

Table 2. The range of target flow rates, sluice gate openings, and weir heights tested in the experiments.

Flow Rate ($10^{-3} \text{ m}^3/\text{s}$)	Sluice Gate Opening (10^{-3} m)	Weir Height (10^{-3} m)
0.5	5	0
1.0	10	10
1.5	15	25
2.0	25	50
2.5	50	100
3.0	100	150

These ranges lead to 216 initial combinations of the three variables. To avoid overflow of the flume, a maximum flow depth of 0.2 m in the channel was considered as a limit to halt and exclude a combination during running of the experiment. Variable combinations that resulted in excessive water depths in the flume were labeled as “overflow” in the records and excluded from testing. Combinations of variables that resulted in the sluice gate having no interactions with the flow (i.e., sluice gate opening is more than flow depth) were excluded from testing. All other possible combinations in which the sluice gate affects the flow were studied and measured. Measurements were collected only once the upstream depth became constant to ensure that the system had achieved steady-state flow. The flows resulting from all the possible variable combinations covered a wide range of sluice gate operating conditions, including free and submerged hydraulic jumps.

2.3. Evaluation Criteria

A combination of visualizations and statistical tests were applied to evaluate and compare lab experiment measurements (observations) with corresponding estimations (predictions) from the studied methods. In the following equations, n is the number of data points, O_i is the observation value, \bar{O} is the average value of the observations, P_i is the estimated value, \bar{P} is the average value of the estimations [35].

The mean error (ME) is defined as the average difference between the model estimations and the experimentally measured value:

$$\text{ME} = \frac{1}{n} \sum_{i=1}^n (P_i - O_i) \quad (31)$$

Mean absolute error (MAE) is the average absolute difference between the model estimations and the experimentally measured values:

$$\text{MAE} = \frac{1}{n} \sum_{i=1}^n |P_i - O_i| \quad (32)$$

The mean percentage error (MPE) is the average of percentage errors (the difference between predicted and measured values) [36] and represents errors in a dimensionless form which is easier to analyze and compare:

$$\text{MPE} = \frac{100}{n} \sum_{i=1}^n \frac{P_i - O_i}{O_i} \quad (33)$$

The mean absolute percentage error (MAPE) is defined as:

$$\text{MAPE} = \frac{100}{n} \sum_{i=1}^n \left| \frac{P_i - O_i}{O_i} \right| \quad (34)$$

and is the average of individual absolute percentage errors and one of the most common accuracy measures [37] recommended in many textbooks (e.g., [36,38]). MAPE considers errors regardless of their sign, so positive and negative errors cannot cancel each other.

3. Results

3.1. Flow Regimes' Distinguishing Conditions

Figure 5 shows the experiment results, with each point representing a measurement. This figure also compares regions of predicted flow regime for each method by providing the distinguishing conditions of each method plotted by dotted lines. For example, all points that fall below the $Y_{D_{MF}}$ curve of the EM model are considered as free flow by this model.

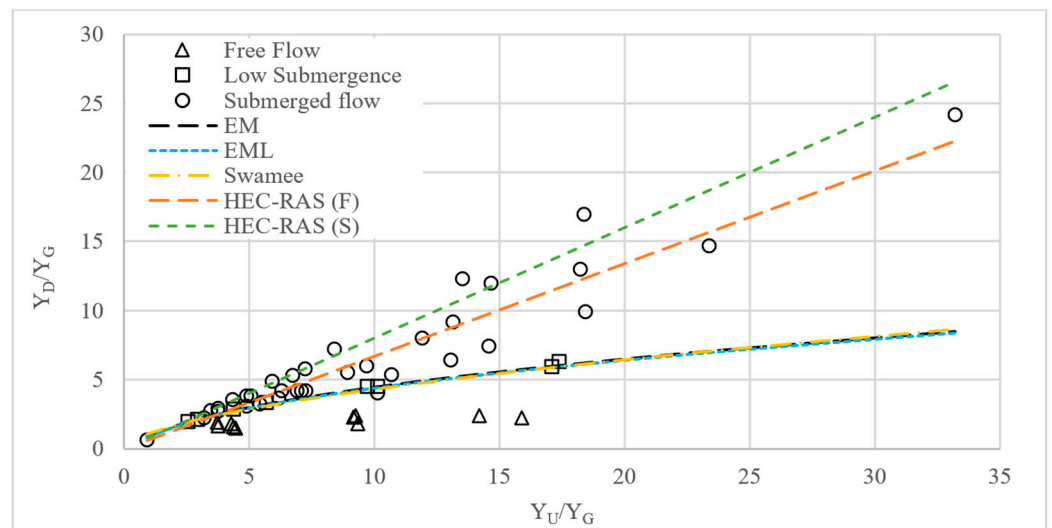


Figure 5. Lab experiment results (markers) categorized by observed flow regime, compared with predicted flow regimes by each model (lines).

3.2. Discharge Coefficient and Flow Rate

The coefficients of discharge (C_d) and volumetric flow rates for the EM, EML, Henry, and Swamee models were estimated using the equations provided in Section 2.1. In order to examine scaling effects on the energy loss factor k , this study applied the loss factor values in Equation (13) reported by Habibzadeh et al. (2011) for the EML. The estimated volumetric flow rate of these models is represented in Figure 6. The summary of evaluation models in estimating the flow rate in each sluice gate operation range is represented in Table 3.

Table 3. The evaluation criteria for estimated flow rates.

Model	Flow	ME (m ³ /s)	MAE (m ³ /s)	MPE (%)	MAPE (%)
EM	F	1.00×10^{-4}	3.15×10^{-4}	12.59	20.38
	S	7.19×10^{-7}	8.32×10^{-5}	-1.65	7.01
EML	F	6.39×10^{-5}	3.38×10^{-4}	11.30	21.23
	S	-3.39×10^{-5}	8.18×10^{-5}	-3.54	7.25
Henry	F	1.31×10^{-4}	3.44×10^{-4}	14.28	21.99
	S	1.72×10^{-4}	2.48×10^{-4}	20.19	25.20
Swamee	F	-1.15×10^{-3}	1.18×10^{-3}	-53.94	57.70
	S	-9.72×10^{-4}	9.72×10^{-4}	-73.59	73.59

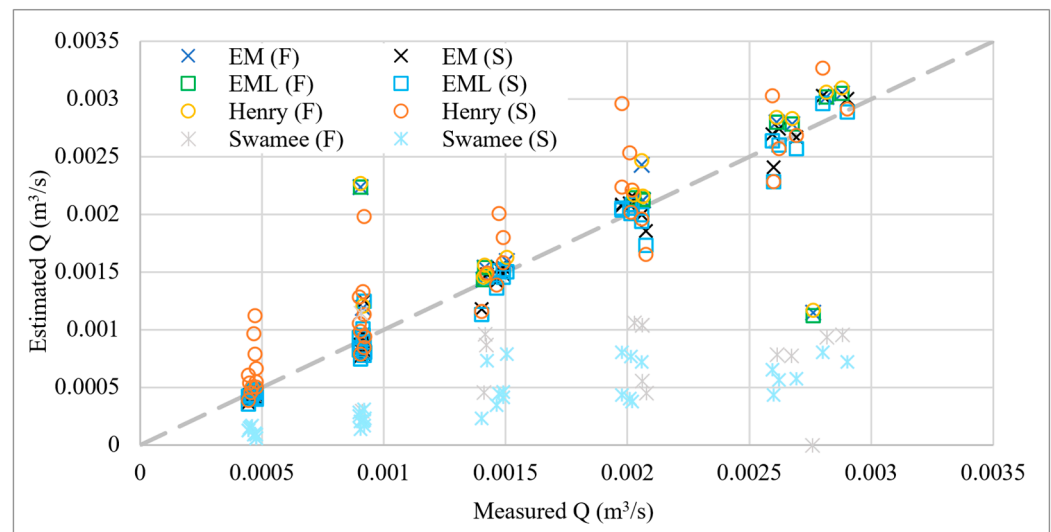


Figure 6. The estimated volumetric flow rate of methods for free and submerged flows.

4. Discussion

4.1. Flow Regimes' Distinguishing Conditions

Based on Figure 5, EM, EML and Swamee's model produced almost identical curves to distinguish free and submerged flows. Uniquely, the HEC-RAS model identifies three zones to distinguish free flow, partially submerged flow, and submerged flows.

Comparing the number of cases that a method succeeds in distinguishing a flow regime to the cases that it fails could help measure each method's accuracy in distinguishing the flow regimes. The EM, EML, Swamee, and HEC-RAS models accurately predicted the observed flow regime 83%, 81%, 86%, and 48%, respectively. Note that these results may underestimate the accuracy of models that do not distinguish partially submerged flow conditions, and the cases that could not be clearly categorized as free flow or submerged flow were considered as erroneous predictions.

These results also suggest that, at least for this laboratory-scale experiment, the HEC-RAS estimations for distinguishing the flow regime are not accurate. According to Equations (4), (5), (17) and (24), the distinguishing measure of the EM, EML and Swamee's models are represented as a function of Y_U and Y_G . However, the HEC-RAS model distinguishing flow regime is only based on Y_U .

4.2. Discharge Coefficient and Flow Rate

Analysis of the experimental results indicates that the contraction coefficient (C_c) in this experiment ranged from 0.576 to 0.623 with an average of 0.591. This range is in good agreement with the 0.58–0.63 range reported by Rajaratnam and Subramanya (1967) [10]. Additionally, this average is very close to the suggested value of 0.6 by Henry (1950) [14] and 0.61 by Henderson (1966) [33] and Rajaratnam and Subramanya (1967) [10], and the value of 0.611 assumed by Swamee (1992) [15].

The evaluation results of studied models in estimating volumetric flow rate represented in Figure 6 and Table 3 indicate a reasonable performance for EM, EML, and Henry's models in free flow. For submerged flow, the performance of EM and EML models were reasonable. The performance of Henry's model was significantly lower than EM-based models for submerged flow. Swamee's model performance was not acceptable for free and submerged flows.

According to Figure 6, Swamee's model estimates the flow rate significantly lower than other models. The poor results of Swamee's (1992) model with the experimental data in this study were consistent with results reported by Sepulveda et al. (2009), Belaud et al. (2009), and Habibzadeh et al. (2011) [18,39,40]. Since EM, EML, Henry, and Swamee models use the same equation to calculate the volumetric flow rate, C_d is the only differing factor in these methods' estimations of volumetric flow rate. Therefore, the volumetric flow rates

could be used to evaluate the efficiency of each method in estimating the coefficient of discharge. Results indicate that the Swamee method’s estimated coefficients of discharge for this experiment are significantly lower than the other methods. Additionally, in a few cases Swamee’s method estimates some imaginary numbers for C_d that are not reasonable. Similar results were reported by Habibzadeh et al. (2011) [18]. Based on these results and considering that the nonlinear regression of Swamee’s (1992) model is based on Henry’s (1950) nomogram could raise concerns about the generality of this method and the effects of scale on its accuracy.

4.3. New Analytical Equations and Methods for Design Purposes

4.3.1. Determination of Loss Factor for the EML Model

Studies such as Silva and Rojo’s (2017) applied the loss factor values in Equation (13) reported by Habibzadeh et al. (2011) [3,18] for the EML model. However, calibrating k using this experimental data showed that for this study, the value of k is 0.184 for free flow and 0.0662 for submerged flow. These results indicate the importance of determining the loss factor k for different scales and cases.

For submerged flow, k could be determined by substituting Equation (15) into Equation (1) and applying numerical methods. For free flow, substituting Equation (14) into Equation (1) or using Equation (11) leads to the following equation for the determination of k :

$$k = \Delta^2 \left(1 + 2 \frac{Y_u^3}{Y_{Cr}^3} (1 - \Delta) \right) - 1 \tag{35}$$

4.3.2. Determination of C_d for the HEC-RAS Model

The HEC-RAS method only offers a recommended range for C_d and does not offer any analytical methods to calculate C_d . When experimental data is available, C_d could be estimated by calibrating the model using the experimental data. However, for design purposes, the application and accuracy of this model, and the HEC-RAS software for sluice gates, will be highly dependent on the operator’s experience and choice. This study offers and evaluates the application of an analytical model based on the EM method to estimate the C_d dynamically for HEC-RAS since it applies the same flow rate equation to the EM method for free flow and relatively similar equations for other conditions.

In this study, three methods were proposed and evaluated and compared for the estimation of C_d for the HEC-RAS model: 1. Calibration, 2. Dynamic method, and 3. Adjusted dynamic method. For the calibration (first) method, there is one C_d for each flow regime range which is calculated using the experimental data. For both dynamic methods, a separate C_d is estimated for each calculation based on the EM equations: Equation (2) for free flow, Equation (8) for submerged flow and the average of free and submerged flow for partially submerged flow. For the adjusted method, the estimated C_d is adjusted to the closest minimum or maximum value of the HEC-RAS recommended range if the calculated value is outside this range. Table 4 represents the calibrated and the average C_d of dynamic and adjusted dynamic models for the flow ranges defined by HEC-RAS. The estimated volumetric flow rate of each method is represented in Figure 7. The evaluation criteria of these estimations are represented in Table 4.

Table 4. The estimated C_d for HEC-RAS and the evaluation criteria for estimated flow rates.

Flow Regime	Free			Partially Submerged			Submerged			
	Method	C_d	MPE (%)	MAPE (%)	C_d	MPE (%)	MAPE (%)	C_d	MPE (%)	MAPE (%)
Calibration		0.506	5.6	12.26	0.688	−7.18	15.04	0.363	0.97	13.30
Dynamic		0.499	3.74	10.53	0.435	3.50	21.59	0.241	−61.49	61.49
Dynamic (Adj.)		0.527	9.95	12.44	0.5	16.84	26.30	0.50	−19.69	23.00

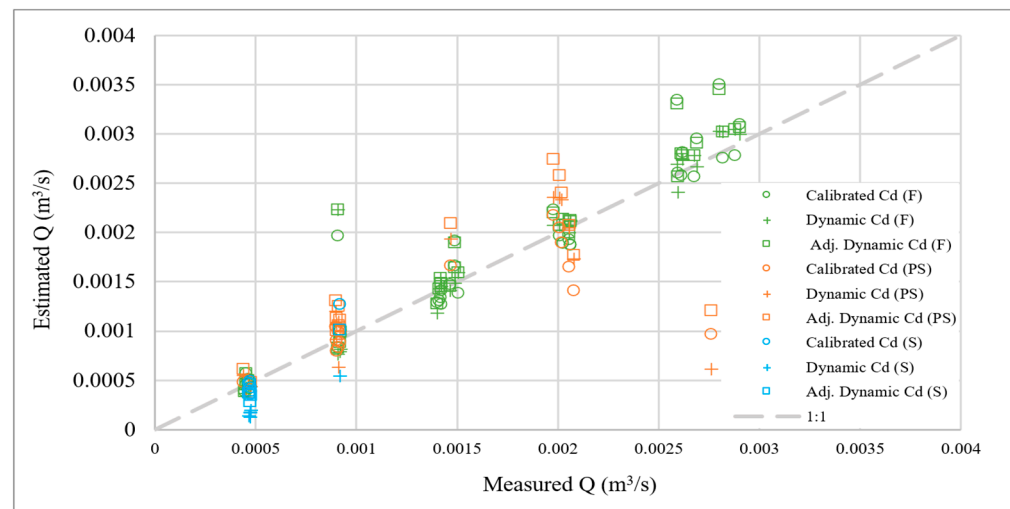


Figure 7. The estimated volumetric flow rate of methods to estimate C_d for HEC-RAS.

4.3.3. Analysis of Improvements

The newly proposed equations and methods were applied to calibrate values of k for the EML model. For the HEC-RAS model, C_d is calculated using the dynamic model for free flow, and partially submerged flow and the adjusted dynamic method is used for the submerged flow.

Results from using the calibrated loss factor k are represented in Table 5. The comparison of the evaluation criteria results represented in Tables 3 and 5 indicates that calibration of loss factor k led to reasonable improvements in the EML model’s accuracy for both free and submerged flow regimes.

Table 5. Evaluation of models in estimating the flow rate in the full sluice gate operation range.

Model	Flow	ME (m³/s)	MAE (m³/s)	MPE (%)	MAPE (%)
EM	F	1.00×10^{-4}	3.15×10^{-4}	12.59	20.38
	S	7.19×10^{-7}	8.32×10^{-5}	−1.65	7.01
EML	F	5.45×10^{-5}	2.76×10^{-4}	5.24	18.00
	S	-1.11×10^{-5}	8.13×10^{-5}	−2.00	7.03
Henry	F	1.31×10^{-4}	3.44×10^{-4}	14.28	21.99
	S	1.72×10^{-4}	2.48×10^{-4}	20.19	25.20
Swamee	F	-1.15×10^{-3}	1.18×10^{-3}	−53.94	57.70
	S	-9.72×10^{-4}	9.72×10^{-4}	−73.59	73.59
HEC-RAS	F	6.60×10^{-5}	1.3×10^{-4}	3.74	10.53
	PS	-1.54×10^{-5}	1.57×10^{-4}	3.50	21.59
	S	-8.59×10^{-5}	1.16×10^{-4}	19.69	23.00

HEC-RAS applies Equation (1) for estimating the volumetric flow rate, which is the same as the EM-based models. Therefore, Equation (2) seems to be a reasonable analytical method for determining C_d for free flow in HEC-RAS model. These results support this hypothesis since, according to Table 4, the dynamic method outperformed other methods with a lower MAPE = 10.53% for free flow. The calibrated C_d led to better performance in estimating the flow rate for partially submerged and submerged flows, resulting in MAPEs of 15.04% and 13.30%, respectively. However, the experimental data are required for calibration. Therefore, for the HEC-RAS model, it may be reasonable to use the dynamic

method to estimate C_d for partially submerged flow and the adjusted dynamic method for submerged flow.

Although HEC-RAS applies a similar equation to estimate flow rate in free flow, results could not be compared with other models since the flow regime distinguishing conditions of HEC-RAS mistakenly considered many submerged flow cases as free flow. It is worth mentioning that for submerged flow, in this experiment, the calibrated $C_d = 0.363$ is significantly lower than the minimum recommended range of C_d suggested by HEC-RAS. Based on these results, the HEC-RAS recommended range for C_d was not practical for this experiment.

Table 5 and Figure 8 summarize these results and compare them with the results of other studied models.

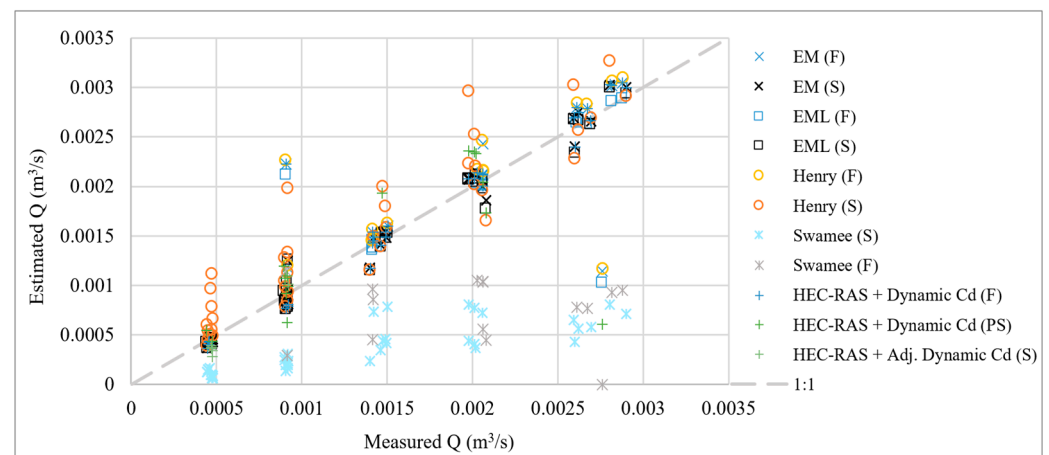


Figure 8. The estimated volumetric flow rate of all models compared to corresponding measured flow rates.

5. Conclusions

Sluice gates are important components in designing, operating, and maintaining water delivery systems and hydropower plants, which are essential elements in the sustainable development of water resources and power generation. This study investigated five models' performances in distinguishing conditions and estimating the coefficient of discharge (C_d) and flow rate in sluice gates for free flow and submerged flows. Experiments in a laboratory flume at the University of Guelph were used to characterize steady-state flow through a sluice gate for different flow rates, gate openings, upstream and downstream conditions. New equations were proposed to make them easier to analyze and compare and facilitate the application of the studied models.

For this experiment, analysis of the EM, EML, and Swamee methods indicated relatively similar curves and performance in distinguishing the sluice gate flow regimes. However, the HEC-RAS model's estimations of the flow regime were not accurate.

Estimating the flow rate results of this experiment indicated a reasonable performance of EM, EML, and Henry's models in free flow. For submerged flow, the performances of EM and EML models were reasonable. The performance of Henry's model was significantly lower than EM-based models for submerged flow. Swamee's models' performance was not acceptable for free and submerged flows. Several other studies report the same issue for this model. The results of this experiment, the fact that the nonlinear regression of Swamee's (1992) method is based on Henry's (1950) nomogram, and similar reports in several studies could raise concerns about the generality of this model and the scaling effects on this method's accuracy. Therefore, it seems that Swamee's (1992) method should be used with extra caution.

This study results also indicated that the scaling effects on loss factor k in the EML model need to be considered for different cases. Investigations showed that calibration k using this experiment data increases the EML accuracy. In practice, most of the losses will

be captured through the calibration of C_d using real field or experiment measurements. For design purposes, the EML model could be considered as a model with reasonable accuracy. Further investigations on this model are recommended.

An analytical equation and method were proposed to determine the loss factor k due to the importance of k in the EML model, which makes it easier to use and improved its performance. Additionally, a new equation form was proposed for the EML model to determine the discharge coefficient in submerged flow.

In addition, a solution was proposed for the HEC-RAS model drawback in not providing any analytical methods to estimate the coefficient of discharge C_d . Technically, C_d could be calibrated when the experimental data is available. However, for design purposes, or when the experimental measurements are not available, such a drawback makes the application and accuracy of HEC-RAS highly dependent on the operator's experience. To address this issue, a method is offered and evaluated to dynamically estimate C_d for HEC-RAS. It led to a reasonable accuracy and enables utilizing this model for design purposes where the experimental data is not available for calibration. Further studies could reveal more facts about this method.

In system optimization, non-iterative and fast analytical calculations for a component are important to maintain the overall efficiency of optimizing the whole system of many components. The new analytical equations, methods, and simplified models presented in this study could assist with modeling sluice gates as a component of complex hydraulic systems, especially when there are many scenarios to be studied, managed, or optimized. Moreover, they could assist where the experimental data is not available for calibration, such as for design purposes or where the flow in open channels needs to be controlled or measured using the sluice gates. This study could benefit the design, optimization, development of management or operation plans, etc., of sluice gates in complex hydraulic systems such as water delivery systems and hydropower plants, which are essential components in the sustainable development of water resources and power generation. Further studies are recommended.

Author Contributions: Conceptualization, A.Y. and W.D.L.; methodology, A.Y. and W.D.L.; software, A.Y.; formal analysis, A.Y.; investigation, A.Y.; resources, W.D.L. and A.Y.; writing—original draft preparation, A.Y.; writing—review and editing, A.Y. and W.D.L.; visualization, A.Y.; supervision, W.D.L.; project administration, W.D.L. and A.Y.; funding acquisition, W.D.L. All authors have read and agreed to the published version of the manuscript.

Funding: This work is part of a larger long-term research program that has been financially supported by the Natural Sciences and Engineering Research Council (NSERC) of Canada, Collaborative Research and Development (CRD) program (grant CRDPJ 513923-17) and Greenbug Energy Inc. (Delhi, Ontario, Canada).

Data Availability Statement: The data used in this study is reported or referenced in the article.

Conflicts of Interest: The authors declare no conflict of interest.

Nomenclature

The following symbols are used in this paper:

A	Area of cross-section	(m ²)
A_i	Area of cross-section i	(m ²)
b	Width of the channel/sluice gate	(m)
C_c	Coefficient of contraction (Y_m/Y_G)	(-)
C_d	Coefficient of discharge	(-)
E_i	Specific energy of the cross-section i	
EM	Energy–Momentum method	
EML	Energy–Momentum method by considering losses	
F	Free flow	
GVF	Gradually varied flow	
g	Gravitational constant	(m/s ²)

k	Loss factor	
M_i	Momentum function of the cross-section i	
MAPE	Mean absolute percentage error	(%)
MPE	Mean percentage error	(%)
Q	Volume flow rate (discharge)	(m ³ /s)
q	Unit discharge ($q = Q/b$)	(m ² /s)
R	Pearson correlation	
S	Submerged flow	
SHJ	Submerged hydraulic jump	
P	Wetted perimeter	(m)
PS	Partially submerged flow	
Y_{Cr}	Critical depth of flow ($\sqrt[3]{q^2/g}$)	(m)
Y_D	Downstream depth	(m)
Y_{DMF}	The maximum downstream depth that a free flow could be expected; the conjugated depth of $Y_m = Y_{J1}$	(m)
Y_G	Gate's opening	(m)
Y_i	Depth of flow at the cross-section i	(m)
\bar{Y}_i	Depth of the centroid of the cross-sectional area from the top of the water surface for the cross-section i	(m)
Y_{J1}	Initial depth of hydraulic jump	(m)
Y_{J2}	Secondary depth of hydraulic jump	(m)
Y_m	The minimum depth of flow after the sluice gate	(m)
Y_P	The piezometric head	(m)
Y_U	Upstream depth	(m)
δ	The upstream to downstream depth ratio (Y_U/Y_D)	(-)
Δ	The ratio of contraction point depth to the upstream depth ($C_c Y_G/Y_U$)	(-)

Appendix A. Hydraulic Background

A classic (free) hydraulic jump is represented in Figure 1. For a specific discharge Q , energy is ideally conserved between sections U and m , and momentum is conserved between sections $J1$ and $J2$. The parameters Y_U and Y_m are called alternate depths and Y_{J1} and Y_{J2} are called conjugate depths. Theoretically, these depths can be estimated using specific energy and momentum methods, respectively. The specific energy at cross-section i is defined as [41]:

$$E_i = Y_i + \frac{Q^2}{2gA_i^2} \quad (A1)$$

where Y_i is the depth of flow, A is the cross-sectional area, and g is the gravitational constant (usually taken as 9.81 m/s²).

In a free hydraulic jump, the jet exiting after the sluice gate rapidly converges until it reaches the “vena contracta,” a point with the minimum cross-sectional area; here, the minimum flow depth Y_m and, as a result, the maximum velocity. This is a region of Rapidly Varied Flow (RVF). For a specific flow rate, if friction can be neglected, the energy between the U and m cross-sections is conserved ($E_U = E_m$) [1], and Y_U and Y_m will be alternative depths, one above the critical depth (Y_U) and the other below it (Y_m). Therefore, for a specific flow rate, Y_U or Y_m could be estimated using Equation (A1) by knowing the other. For rectangular channels with the width b and specific discharge $q = Q/b$ this equation can be simplified as:

$$Y_U + \frac{q^2}{2gY_U^2} = Y_m + \frac{q^2}{2gY_m^2} \quad (A2)$$

In free flow, solving Equation (A2) for q enables calculating the volumetric flow rate using Y_U and Y_m :

$$Q = bY_U Y_m \sqrt{\frac{2g}{Y_U + Y_m}} \quad (A3)$$

In sluice gates, the subcritical upstream flow gradually accelerates to critical near the gate opening and goes to supercritical; then, it comes back to subcritical further downstream after a hydraulic jump is formed [1]. A hydraulic jump is defined as a jump or standing wave that forms when the flow regime rapidly changes from a supercritical to a subcritical state. During this rapid transition, the supercritical upstream flow depth rises quickly to a subcritical depth downstream. The jump may be distinguished by surface rollers, mixing or air entrainment, leading to significant energy dissipation.

For any cross-sectional shape, at cross-section i , the momentum function M_i is defined as [41]:

$$M_i = A_i \bar{Y}_i + \frac{Q^2}{g A_i} \quad (\text{A4})$$

The momentum function (M_i) is conserved at cross-sections $J1$ and $J2$ ($M_{J1} = M_{J2}$). The pair of depths before (Y_{J1}) and after the hydraulic jump (Y_{J2}) are known as conjugate depths [41]. Theoretically, a hydraulic jump forms where the initial and secondary depths satisfy the condition $M_{J1} = M_{J2}$ [31]. For rectangular channels the centroid of a flow at depth Y is located at $\bar{Y} = Y/2$, and Equation (A4) can be simplified to:

$$\frac{Y_{J1}^2}{2} + \frac{q^2}{Y_{J1}g} = \frac{Y_{J2}^2}{2} + \frac{q^2}{Y_{J2}g} \quad (\text{A5})$$

For a specific flow rate, solving Equation (A5) for either Y_{J1} or Y_{J2} results in the following equation that enables finding the conjugate depths by knowing either of them.

$$Y_a = \frac{Y_b}{2} \left(\sqrt{1 + 8 \frac{q^2}{g Y_b^3}} - 1 \right) = \frac{Y_b}{2} \left(\sqrt{1 + 8 Fr_b^2} - 1 \right) \quad (\text{A6})$$

where a and b are $J1$ and $J2$, or vice versa. In practice, the type of hydraulic jump in sluice gates is conditioned by the depth of flow downstream, which depends on the channel slope and roughness as well as obstacles [42].

The flow under sluice gates can be described analytically using energy–momentum concepts. Theoretically, the presence of a sluice gate leads to a hydraulic jump if its opening (Y_G) is less than the critical depth of the flow passing under the gate (Y_{Cr}). The critical depth occurs where the Froude number ($Fr = V / \sqrt{gD}$, where $D = A/T$) is equal to 1. Solving $Fr = 1$ for any cross-section area A and wetted perimeter T leads to the following equation. Therefore, the flow depth is critical if it satisfies the following equation:

$$\frac{Q^2}{g} = \frac{A^3}{T} \quad (\text{A7})$$

For rectangular channels, critical flow depth can be calculated using a simplified form of this equation:

$$Y_{Cr} = \sqrt[3]{q^2/g} \quad (\text{A8})$$

References

1. White, F.M. *Fluid Mechanics*, 7th ed.; McGraw-Hill: New York, NY, USA, 2011; ISBN 978-0073529349.
2. Erbsti, P.C.F. *Design of Hydraulic Gates*, 2nd ed.; CRC Press/Balkema: Boca Raton, FL, USA, 2014; ISBN 0415659396.
3. Silva, C.O.; Rijo, M. Flow Rate Measurements under Sluice Gates. *J. Irrig. Drain. Eng.* **2017**, *143*, 06017001. [CrossRef]
4. Sepúlveda Toepfer, C.A. Instrumentation, Model Identification and Control of an Experimental Irrigation Canal. Ph.D. Thesis, Technical University of Catalonia, Barcelona, Spain, 2007. Available online: https://web.archive.org/web/20211214013540/https://www.tdx.cat/bitstream/handle/10803/5951/01_Sepulveda.pdf (accessed on 14 December 2021).
5. Lewin, J. *Hydraulic Gates and Valves: In Free Surface Flow and Submerged Outlets*; Thomas Telford: London, UK, 1995; ISBN 0727720201.
6. Baume, J.P.; Malaterre, P.O.; Gilles, B.; Benoit, L.G. SIC: A 1D hydrodynamic model for river and irrigation canal modelling and regulation. In *Métodos Numéricos em Recursos Hídricos*; Associação Brasileira de Recursos Hídricos: Porto Alegre, Brazil, 2005.

7. Brunner, G.W. *HEC-RAS River Analysis System Hydraulic Reference Manual—Version 5.0*; no. February; US Army Corps of Engineers Hydrologic Engineering Center: Davis, CA, USA, 2016.
8. Kindsvater, C.E. The Hydraulic Jump in Sloping Channels. *Trans. Am. Soc. Civ. Eng.* **1944**, *109*, 1107–1120. [[CrossRef](#)]
9. Bradley, J.N.; Peterka, A.J. The hydraulic design of stilling basins: Hydraulic jumps on a horizontal apron (basin i). *J. Hydraul. Div.* **1957**, *83*, 1–24. [[CrossRef](#)]
10. Rajaratnam, N.; Subramanya, K. Flow equation for the sluice gate. *J. Irrig. Drain. Div.* **1967**, *93*, 167–186. [[CrossRef](#)]
11. Hager, W.H. Classical Hydraulic Jump. In *Energy Dissipators and Hydraulic Jump*; Kluwer Academic: Dordrecht, The Netherlands, 1992; Volume 8, pp. 5–40, ISBN 0-7923-1508-1.
12. Mahtabi, G.; Chaplot, B.; Azamathulla, H.M.; Pal, M. Classification of Hydraulic Jump in Rough Beds. *Water* **2020**, *12*, 2249. [[CrossRef](#)]
13. Bijankhan, M.; Ferro, V.; Kouchakzadeh, S. New stage-discharge relationships for free and submerged sluice gates. *Flow Meas. Instrum.* **2012**, *28*, 50–56. [[CrossRef](#)]
14. Henry, R. Discussion to ‘On submerged jets’. *Trans. Am. Soc. Civ. Eng.* **1950**, *115*, 687–694.
15. Swamee, P.K. Sluice-Gate Discharge Equations. *J. Irrig. Drain. Eng.* **1992**, *118*, 56–60. [[CrossRef](#)]
16. Roth, A.; Hager, W.H. Underflow of standard sluice gate. *Exp. Fluids* **1999**, *27*, 339–350. [[CrossRef](#)]
17. Lozano, D.; Mateos, L.; Merkley, G.P.; Clemmens, A.J. Field Calibration of Submerged Sluice Gates in Irrigation Canals. *J. Irrig. Drain. Eng.* **2009**, *135*, 763–772. [[CrossRef](#)]
18. Habibzadeh, A.; Vatankhah, A.R.; Rajaratnam, N. Role of Energy Loss on Discharge Characteristics of Sluice Gates. *J. Hydraul. Eng.* **2011**, *137*, 1079–1084. [[CrossRef](#)]
19. Castro-Orgaz, O.; Lozano, D.; Mateos, L. Energy and Momentum Velocity Coefficients for Calibrating Submerged Sluice Gates in Irrigation Canals. *J. Irrig. Drain. Eng.* **2010**, *136*, 610–616. [[CrossRef](#)]
20. Castro-Orgaz, O.; Mateos, L.; Dey, S. Revisiting the Energy-Momentum Method for Rating Vertical Sluice Gates under Submerged Flow Conditions. *J. Irrig. Drain. Eng.* **2013**, *139*, 325–335. [[CrossRef](#)]
21. Gumus, V.; Simsek, O.; Soydan, N.G.; Akoz, M.S.; Kirkgoz, M.S. Numerical Modeling of Submerged Hydraulic Jump from a Sluice Gate. *J. Irrig. Drain. Eng.* **2016**, *142*, 04015037. [[CrossRef](#)]
22. Rady, R.A.E.H. Modeling of flow characteristics beneath vertical and inclined sluice gates using artificial neural networks. *Ain Shams Eng. J.* **2016**, *7*, 917–924. [[CrossRef](#)]
23. Boiten, W. *Vertical Gates for Distribution of Irrigation Water*; Report 30; Delft Hydraulics and Wageningen Agricultural University: Delft, The Netherlands, 1992.
24. Kubrak, E.; Kubrak, J.; Kiczko, A.; Kubrak, M. Flow measurements using a sluice gate; Analysis of applicability. *Water* **2020**, *12*, 819. [[CrossRef](#)]
25. Nasrabadi, M.; Mehri, Y.; Ghassemi, A.; Omid, M.H. Predicting submerged hydraulic jump characteristics using machine learning methods. *Water Supply* **2021**, *21*, 4180–4194. [[CrossRef](#)]
26. Lencastre, A. *Hidráulica Geral [General Hydraulics]*; Edição Luso-Brasileira: Lisbon, Portugal, 1983. (In Portuguese)
27. YoosefDoost, A.; Lubitz, W.D. Design Guideline for Hydropower Plants Using One or Multiple Archimedes Screws. *Processes* **2021**, *9*, 2128. [[CrossRef](#)]
28. YoosefDoost, A.; Lubitz, W.D. Archimedes Screw Design: An Analytical Model for Rapid Estimation of Archimedes Screw Geometry. *Energies* **2021**, *14*, 7812. [[CrossRef](#)]
29. Katopodes, N.D. Ideal Fluid Flow. In *Free-Surface Flow*; Elsevier: Oxford, UK, 2019; pp. 428–515, ISBN 978-0-12-815489-2.
30. AMS Contraction Coefficient—Glossary of Meteorology. American Meteorological Society, 2012. Available online: https://glossary.ametsoc.org/wiki/Contraction_coefficient (accessed on 26 January 2021).
31. Chaudhry, M.H. *Open-Channel Flow*, 2nd ed.; Springer: Boston, MA, USA, 2008; ISBN 9780387686486.
32. Lin, C.H.; Yen, J.F.; Tsai, C.T. Influence of Sluice Gate Contraction Coefficient on Distinguishing Condition. *J. Irrig. Drain. Eng.* **2002**, *128*, 249–252. [[CrossRef](#)]
33. Henderson, F.M. *Open Channel Flow*; Macmillan: New York, NY, USA, 1966; ISBN 9780023535109.
34. Rajaratnam, N.; Subramanya, K. Flow immediately below submerged sluice gate. *J. Hydraul. Div.* **1967**, *93*, 57–77. [[CrossRef](#)]
35. YoosefDoost, A.; Lubitz, W.D. Development of an Equation for the Volume of Flow Passing Through an Archimedes Screw Turbine. In *Sustaining Tomorrow*; Ting, D.S.-K., Vassel-Be-Hagh, A., Eds.; Springer: Cham, Switzerland, 2021; pp. 17–37, ISBN 978-3-030-64715-5.
36. Hanke, J.E.; Wichern, D. *Business Forecasting*, 9th ed.; Prentice Hall: London, UK, 2009; ISBN 978-0132301206. Available online: https://www.google.ca/books/edition/Business_Forecasting/WaiOrL8oct4C?hl=en&gbpv=1&printsec=frontcover (accessed on 15 June 2020).
37. Kim, S.; Kim, H. A new metric of absolute percentage error for intermittent demand forecasts. *Int. J. Forecast.* **2016**, *32*, 669–679. [[CrossRef](#)]
38. Bowerman, B.L.; O’Connell, R.T.; Koehler, A.B. *Forecasting, Time Series, and Regression: An Applied Approach*, 4th ed.; Duxbury advanced series in statistics and decision sciences; Thomson Brooks/Cole: Belmont, CA, USA, 2005; ISBN 9780534409777.
39. Sepúlveda, C.; Gómez, M.; Rodellar, J. Benchmark of Discharge Calibration Methods for Submerged Sluice Gates. *J. Irrig. Drain. Eng.* **2009**, *135*, 676–682. [[CrossRef](#)]

-
40. Belaud, G.; Cassan, L.; Baume, J.-P. Calculation of Contraction Coefficient under Sluice Gates and Application to Discharge Measurement. *J. Hydraul. Eng.* **2009**, *135*, 1086–1091. [[CrossRef](#)]
 41. Moglen, G.E. *Fundamentals of Open Channel Flow*; CRC Press (Taylor & Francis Group): Boca Raton, FL, USA; London, UK; New York, NY, USA, 2015; ISBN 9781466580077.
 42. Raju, K.G.R. *Flow through Open Channels*; TATA McGraw-Hill Publishing Company Limited: New Delhi, India, 1981.